

Effect of frequency and applied voltage of an atmospheric-pressure dielectric-barrier discharge on breakdown and hydroxyl-radical generation with a liquid electrode

Cite as: J. Vac. Sci. Technol. A **38**, 043001 (2020); <https://doi.org/10.1116/6.0000125>

Submitted: 15 February 2020 . Accepted: 30 April 2020 . Published Online: 20 May 2020

Joshua M. Blatz, Daniel Benjamin, Faraz A. Choudhury, Benjamin B. Minkoff, Michael R. Sussman, and J. Leon Shohet

COLLECTIONS

Paper published as part of the special topic on [Special Topic Collection Commemorating the Career of John Coburn](#)
Note: This paper is part of the Special Topic Collection Commemorating the Career of John Coburn.



View Online



Export Citation



CrossMark

ARTICLES YOU MAY BE INTERESTED IN

[Role of organic molecules in enabling modern technology](#)

Journal of Vacuum Science & Technology A **38**, 043201 (2020); <https://doi.org/10.1116/6.0000099>

[Influence of precursor dose and residence time on the growth rate and uniformity of vanadium dioxide thin films by atomic layer deposition](#)

Journal of Vacuum Science & Technology A **38**, 042401 (2020); <https://doi.org/10.1116/6.0000152>

[The role of plasma in plasma-enhanced atomic layer deposition of crystalline films](#)

Journal of Vacuum Science & Technology A **38**, 040801 (2020); <https://doi.org/10.1116/6.0000145>



Instruments for Advanced Science

Contact Hiden Analytical for further details:
www.HidenAnalytical.com
info@hiden.co.uk
[CLICK TO VIEW](#) our product catalogue

Gas Analysis	Surface Science	Plasma Diagnostics	Vacuum Analysis
 <ul style="list-style-type: none">dynamic measurement of reaction gas streamscatalysis and thermal analysismolecular beam studiesdissolved species probesfermentation, environmental and ecological studies	 <ul style="list-style-type: none">UHV/TPOSIMSend point detection in ion beam etchelemental imaging - surface mapping	 <ul style="list-style-type: none">plasma source characterizationetch and deposition process reaction kinetic studiesanalysis of neutral and radical species	 <ul style="list-style-type: none">partial pressure measurement and control of process gasesreactive sputter process controlvacuum diagnosticsvacuum coating process monitoring



Effect of frequency and applied voltage of an atmospheric-pressure dielectric-barrier discharge on breakdown and hydroxyl-radical generation with a liquid electrode

Cite as: J. Vac. Sci. Technol. A 38, 043001 (2020); doi: 10.1116/6.0000125

Submitted: 15 February 2020 · Accepted: 30 April 2020 ·

Published Online: 20 May 2020



View Online



Export Citation



CrossMark

Joshua M. Blatz,¹ Daniel Benjamin,¹ Faraz A. Choudhury,² Benjamin B. Minkoff,² Michael R. Sussman,² and J. Leon Shohet^{1,a)}

AFFILIATIONS

¹Department of Electrical and Computer Engineering, University of Wisconsin–Madison, Madison, Wisconsin 53706

²Department of Biochemistry, University of Wisconsin–Madison, Madison, Wisconsin 53706

Note: This paper is part of the Special Topic Collection Commemorating the Career of John Coburn.

^{a)}Electronic mail: shohet@engr.wisc.edu

ABSTRACT

This work examines the effect of the frequency and peak applied voltage on hydroxyl-radical generation in a dielectric-barrier plasma discharge between a metallic needle electrode and one electrode covered with dielectric. The authors examine a system that can expose up to 96 liquid samples in an automated fashion without human intervention beyond setting the initial software configuration. Then, hydroxyl-radical concentration, measured through coumarin fluorescence, was measured for 5 s plasma exposures generated under different high-voltage conditions with frequencies from 2 to 16 kHz and amplitudes from 4 to 9 kV. Their results show that an increase in frequency and/or applied voltage, within the range prescribed above and the limits of the high-voltage power supply, can yield up to a 150% increase in fluorescence with an equivalent hydroxyl-radical increase. Applications using typical previous methods, such as the Fenton Reaction, are limited in that they continuously generate hydroxyl radicals over millisecond and longer intervals. These results establish the electrical parameters that can now be applied to polymers, like proteins, which show three dimensional structures that are flexible and fluctuate on a microsecond and nanosecond time scale, with hydroxyl-radical generation on this time scale using this device. Additionally, plasma exposures may be optimized for a great variety of proteins, devices and techniques, where hydroxyl-radical generation is of utmost importance, reducing exposure time and potential subjection of samples to harmful side effects.

Published under license by AVS. <https://doi.org/10.1116/6.0000125>

I. INTRODUCTION

The intersection of plasma physics, biotechnology, and medicine, collectively known as plasma medicine, has recently yielded many powerful new tools and techniques related to plasma-activated media, wound healing, and disinfection of medical-instrumentation.¹ These discoveries leverage the unique properties of plasma such as atmospheric-pressure operation, “cold-plasma” discharges, and the ability to generate photons, radicals, as well as charged and neutral molecules. One technique recently developed by our group is PLasma-Induced Modification of Biomolecules or PLIMB.² Here, hydroxyl radicals are generated

with a dielectric barrier discharge³ (DBD), which reacts with solubilized proteins or biomolecules (Fig. 1). This is accomplished by suspending a metal-needle electrode 1 mm above a liquid solution. The potential of the needle electrode is sinusoidally modulated to thousands of volts, causing a plasma to form in the air gap between the needle and the liquid. This plasma self-extinguishes within hundreds of nanoseconds, generating very short bursts of hydroxyl radicals. This is particularly useful for studying protein structure, conformation, and dynamics by employing a process known as hydroxyl-radical footprinting (HRF).⁴ HRF uses highly reactive hydroxyl radicals to react with the water-soluble regions of the

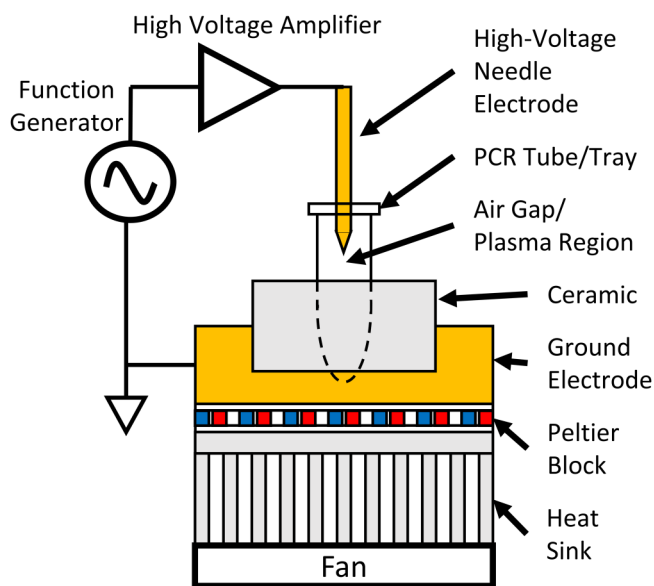


FIG. 1. Schematic of the PLIMB DBD system.

protein followed by mass spectrometry (MS) to gain insight into protein structure as well as protein-protein or protein-small molecule binding information.

In previous PLIMB work, the peak applied voltage and frequency used to generate the plasma in air were initially held constant over a liquid containing various proteins.² While this was able to generate hydroxyl radicals and achieve useful results, it was previously unknown if changing these electrical parameters would modify hydroxyl-radical generation and/or interaction with biological molecules. Additionally, one advantage of using an atmospheric-pressure plasma is that radical generation is possible using inexpensive and widely available high-voltage transformers like those used in neon signs. However, these power sources often operate at fixed voltages and frequencies, limiting the range of electrical parameters that may be varied. In this work, we use PLIMB and the flexibility associated with using a variable frequency high-voltage amplifier to examine the effects that variation of the applied voltage and frequency have on hydroxyl-radical generation during pulsed-plasma operation.

II. MATERIALS AND METHODS

All samples were exposed using a multiplexing system. This system has the ability to expose up to 96 samples in one experiment with minimal user interaction, thus reducing variability due to human or device errors and handling.

To generate the DBD, a nickel-coated steel needle was attached to x- and z-axis translational stages (Thorlabs NRT150 and Thorlabs ZFS25B, respectively) with a $2.5 \times 2.5 \times 15 \text{ cm}^3$ piece of acrylic, which also acts as a high-voltage dielectric. The samples are dispensed into a 96-well 0.25 ml disposable polymerase chain reaction (PCR) tray that fits into a thermally conductive, electrically

insulating ceramic, fabricated from Shapal Hi-M Soft. This sits atop a Peltier cooler and y-axis translational stage (Thorlabs NRT100).

Custom LABVIEW software was written to enable control of each translational stage and an HP 8116A programmable pulse/function generator. This software allows well-to-well control of the frequency and amplitude of the electrical signal applied to the needle electrode as well as control of plasma exposure duration to within 20 ms.

During exposure, the current and applied voltage at the needle electrode were measured using a Pearson 110 current monitor and a Tektronix P6015A high-voltage probe. This information was captured using a LeCroy LC574AL oscilloscope.

Samples were prepared by dissolving coumarin (Sigma C4261) in water at 1 mM concentration. One hundred microliter (μl) samples (aliquots) were dispensed into the 96-well PCR plates and chilled to 2°C for the entire exposure duration.

Measurement of the fluorescence of the plasma-exposed coumarin solution, which is an indicator of hydroxyl generation, was carried out using a Tecan SPECTRAFluor Plus fluorometer. Similar to those used by Louit *et al.*,⁵ an excitation wavelength of 365 nm was used with emission measured at 460 nm.

III. RESULTS

A. Coumarin can be used as a hydroxyl-radical detector

It is well known that atmospheric-pressure DBD plasmas are able to generate hydroxyl radicals in solution.¹ These hydroxyl radicals are thought to be generated via UV photolysis.⁶ To measure radical generation, coumarin was solubilized in water. When coumarin and hydroxyl radicals react, the fluorescent molecule umbelliferone is formed.⁵ While coumarin may also react with other reactive oxygen species, Louit *et al.* “have demonstrated that coumarin shows good selectivity toward the HO^* .” Because coumarin has good hydroxyl-radical selectivity, the fluorescence of plasma-exposed coumarin is a useful indicator of hydroxyl-radical generation. Figure 2 shows a representative selection of fluorescent intensity versus plasma exposure time.

From this figure, we see that as plasma exposure time increases, the fluorescence initially increases but then reaches a peak and falls. This behavior is likely due to multiple effects including the formation of nonumbelliferone coumarin derivatives as well as the fragmentation of coumarin and its derivatives by the plasma. In addition to hydroxyl radicals, an atmospheric-pressure plasma in air, along with water vapor, can also generate a variety of other species including nitric and nitrous acids, which cause the solution pH to drop.⁷ This is important because umbelliferone becomes successively more protonated at lower pH, causing a decrease in fluorescence.⁸ To avoid these complications and restrict coumarin fluorescence to the linear-increasing region, all plasma exposures were held constant at 5 s. As seen in our previous work, time-averaged hydroxyl-radical generation in PLIMB is linear with respect to time, necessitating this restriction.²

B. Multiplex system is repeatable

Our previous work made use of a single-well exposure system that, after each exposure, the sample had to be manually replaced

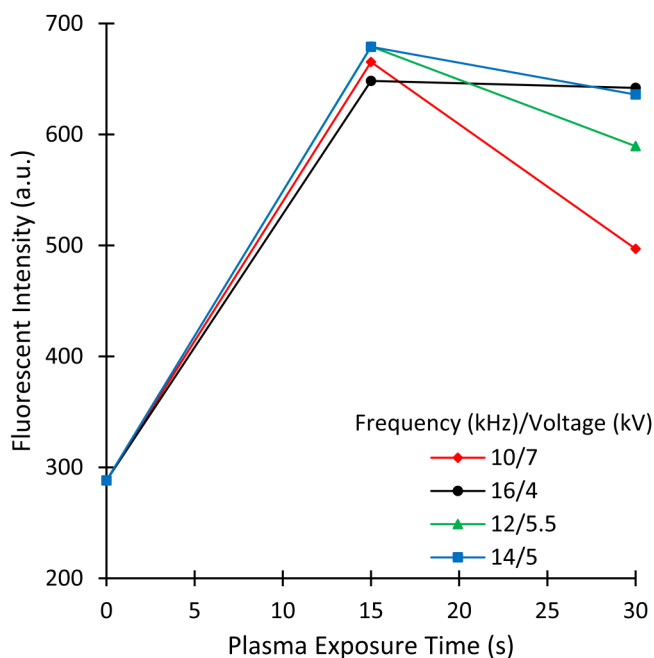


FIG. 2. Fluorescence of plasma-exposed coumarin solution vs plasma exposure time at several frequency and applied voltage amplitudes.

with the next sample.² To minimize error, a multiplexing system was built in which a 96-well PCR plate, shown in Fig. 3, could be filled with samples, cooled, and the needle electrode sequentially and automatically lowered into each well. To test the reproducibility of this system, each of the 96 wells was filled with 100 μ l of 1 mM coumarin solution and exposed for 5 s with 5 kV applied voltage amplitude at a frequency of 10 kHz.

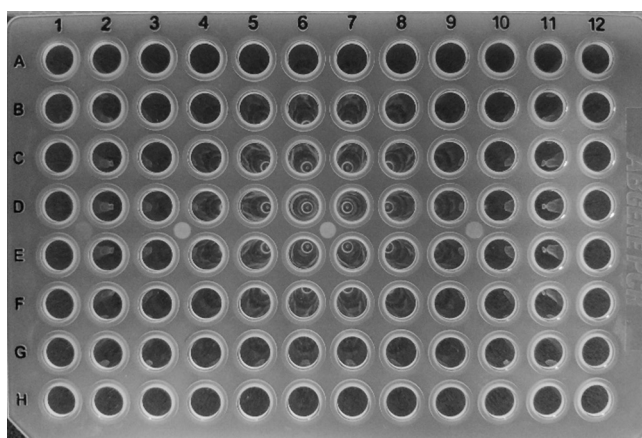


FIG. 3. Picture of the 96-well PCR plates used in the PLIMB multiplex system.

From Table I, it can be seen that while the interior wells (2–11 and B–G) show consistent fluorescent results, the exterior wells exhibited decreased fluorescence indicating less hydroxyl-radical generation in those locations. The fluorescence of the interior 60 wells yields a standard deviation (SD) of 8.15, which is a 60% improvement over the 13.8 SD for the entire 96 wells. As such, all exposures were restricted to the inner 60 wells to maintain uniform-exposure conditions.

It is possible that the loss in hydroxyl-radical generation could be due to geometric-edge effects. Each of the interior wells has eight neighboring wells, while the exterior wells have between three and five neighboring wells. This change in nearby geometry may affect the electric field during the plasma discharge and cause negative effects on hydroxyl-radical generation.

C. Increase in frequency and/or applied voltage increases the rate of hydroxyl-radical generation

To determine the effect the variations of the frequency and peak applied voltage used to generate the plasma have on hydroxyl-radical generation in a fixed amount of time, a two-dimensional array of frequencies and applied voltages was used. Five seconds was chosen as the plasma exposure time to restrict coumarin fluorescence to its linear region. Peak applied voltage was varied from ± 4 to ± 9 kV in 1 kV increments. The frequency was set between 2 and 16 kHz in 2 kHz increments. Because 10 kHz and 10 kV peak-to-peak are the conditions of previous published work,² particular attention was given to results around those conditions; hence, the inclusion of combinations of ± 4.5 kV, ± 5.5 kV, 9 kHz, and 11 kHz. Each combination of frequency and applied voltage was tested in triplicate with fluorescent intensity used as a measure of hydroxyl-radical generation and is presented in Table II. Note that not all combinations of frequency and peak applied voltage were attainable due to amplifier and/or physical limitations.

In addition to limiting exposures to the inner wells of the multiplex system, all combinations of frequency and peak applied voltage were randomized with respect to well location to remove any residual bias. From Table II, we can relate the fluorescent intensity (F) of plasma-exposed coumarin solution as a function of both electrical frequency (f) and applied voltage (v) by fitting a

TABLE I. Fluorescence intensity (arbitrary units) of plasma-exposed coumarin solution after 5 s of ± 5 kV/10 kHz exposure per well in a 96-well PCR plate. Each combination of letter (A–H) and number (1–12) represents a single well in the PCR plate.

	1	2	3	4	5	6	7	8	9	10	11	12
A	314	304	309	315	297	306	303	305	318	308	309	282
B	273	302	305	305	308	304	311	306	293	309	324	305
C	287	320	309	319	300	302	312	312	321	314	321	292
D	272	306	314	305	308	308	303	308	302	317	297	315
E	288	309	311	322	306	312	315	315	312	309	328	270
F	278	315	311	320	305	313	312	314	297	321	323	301
G	293	321	337	324	307	318	316	309	316	305	316	258
H	262	289	301	302	297	308	303	305	286	317	325	309

TABLE II. Fluorescence of plasma-exposed coumarin solution, in arbitrary units, as a function of peak applied voltage (horizontal axis) and frequency (vertical axis). The value following the \pm indicates the spread in fluorescence intensity as measured from three different plasma exposures at those conditions.

Frequency (kHz)	Peak applied voltage (kV)							
	± 4	± 4.5	± 5	± 5.5	± 6	± 7	± 8	± 9
2	317 ± 0		299 ± 12		327 ± 18	352 ± 5	352 ± 11	362 ± 11
4	308 ± 15		349 ± 7		348 ± 13	358 ± 11	375 ± 7	427 ± 0
6	314 ± 12		354 ± 9		334 ± 19	400 ± 0	430 ± 12	460 ± 3
8	351 ± 8		381 ± 15		404 ± 18	398 ± 17		
9		384 ± 6	376 ± 8	386 ± 11				
10	348 ± 3	379 ± 14	417 ± 2	389 ± 13	425 ± 13	422 ± 6		
11		420 ± 6	412 ± 0	430 ± 7				
12	391 ± 6		392 ± 8	406 ± 5				
14	388 ± 7		410 ± 7					
15		405 ± 17						
16	413 ± 17							

linear multivariate equation. The result yields

$$F(f, v) = 194.65 + 9.37f + 19.81v. \quad (1)$$

Figure 4 is a plot of measured coumarin fluorescence versus calculated coumarin fluorescence using Eq. (1). A dashed line has

been added to represent perfect correlation between measured and calculated fluorescence. As can be seen, the data points cluster along the dashed line indicating a strong correlation between the dependent variable, fluorescence (arbitrary units), and both independent variables, frequency (kHz) and applied voltage amplitude (kV).

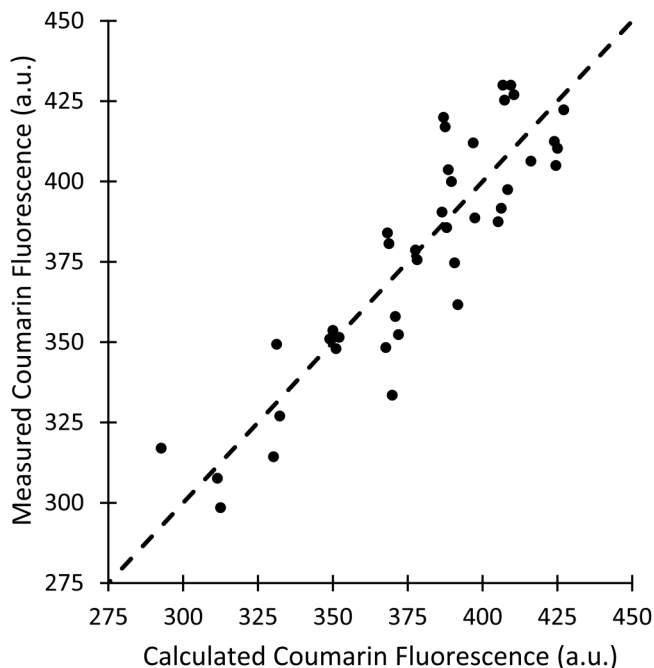


FIG. 4. Measured coumarin fluorescence vs calculated coumarin fluorescence using Eq. (1).

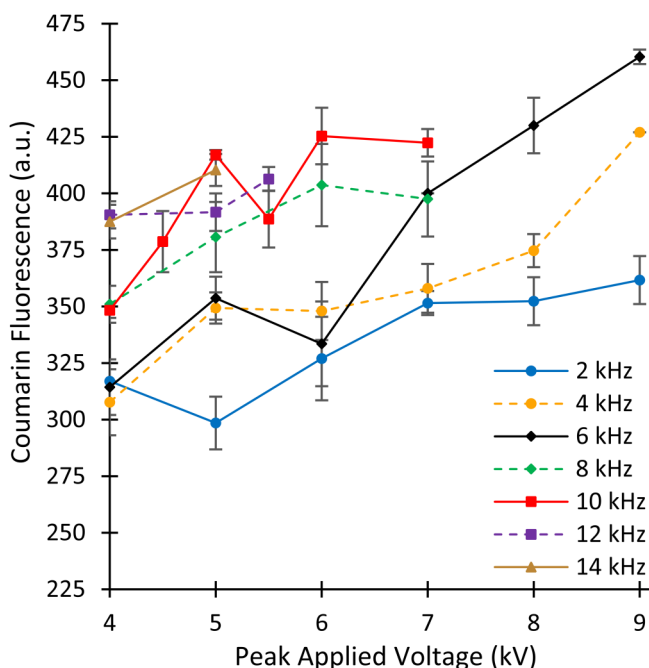


FIG. 5. Fluorescence intensity of 5-s plasma-exposed coumarin solution as a function of applied voltage amplitude with frequency as a parameter.

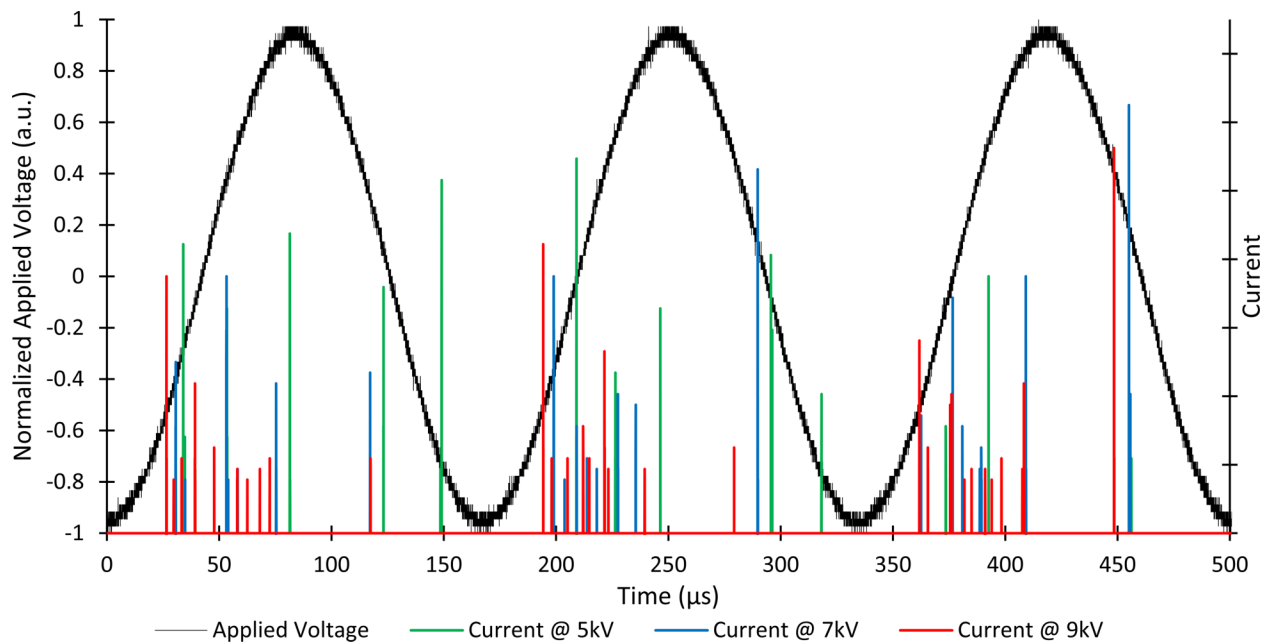


FIG. 6. Current and applied voltage, with respect to ground, at the needle electrode during plasma discharge at a constant frequency of 6 kHz.

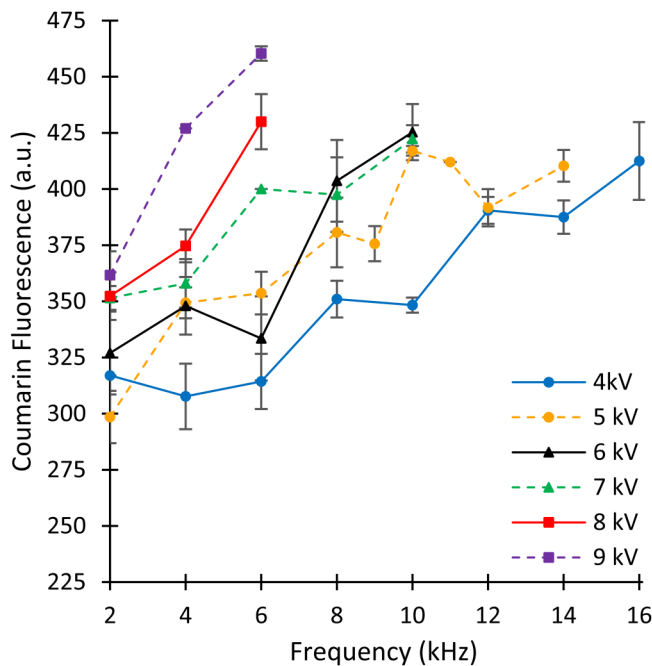


FIG. 7. Fluorescence intensity of 5-s plasma-exposed coumarin solution as a function of frequency with applied voltage amplitude as a parameter.

IV. DISCUSSION

A. Increase in applied voltage results in an increase in hydroxyl-radical generation

First, we will examine the effect of applied voltage on hydroxyl-radical generation. Figure 5 presents fluorescence intensity versus peak applied voltage with frequency as a parameter, taken from Table II.

From this figure, we can see that as applied voltage increases, coumarin fluorescence generally increases implying that hydroxyl-radical generation also increases. To understand why, we examine the current at the needle electrode versus time.

The applied voltage shown in Fig. 6 is the voltage applied at the needle, which has been normalized with respect to the peak voltage conditions and with each spike in current corresponding to a plasma discharge. Figure 6 shows that as the peak applied voltage increases, the number of breakdowns in a single period, and thus the number in a fixed amount of time, increases.

This can occur due to the breakdown mechanism of the DBD. A breakdown will occur when the potential across the air gap, between the needle and the liquid/dielectric surface, exceeds dielectric strength of air. When this occurs, the insulating air gap becomes a conductive plasma. Charged particles will flow through the plasma with direction dictated by the electric field across the air gap. This causes the liquid surface to charge, reducing the potential across the air gap and quickly extinguishing the plasma. With the plasma extinguished, the potential across the air gap can again

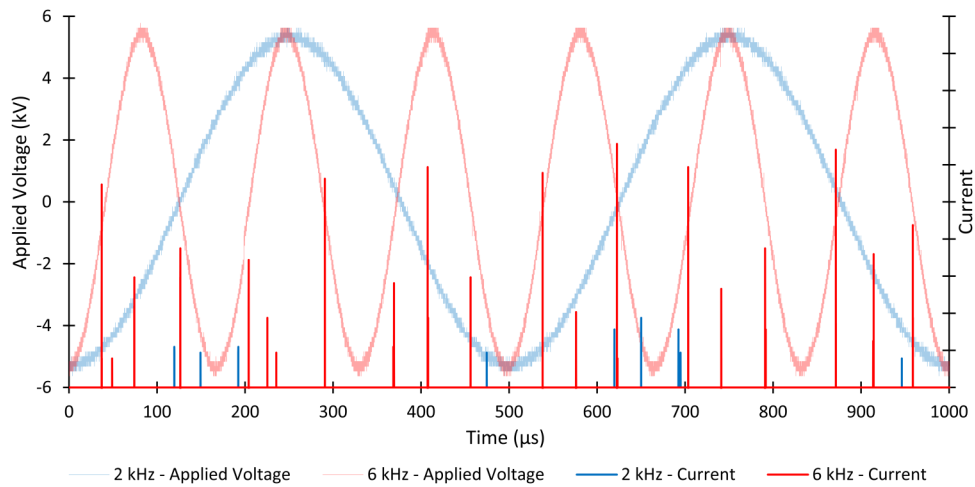


FIG. 8. Current and applied voltage, with respect to ground, at the needle electrode during plasma discharge at 2 kHz (blue) and 6 kHz (red) frequencies with constant ± 5 kV peak voltage.

increase and further breakdowns can occur. When using a higher applied voltage, this breakdown process may occur more often during a single upward or downward voltage shift, as compared to a smaller applied voltage.

B. Increasing frequency increases hydroxyl-radical generation

Next, we examine the effect of varying frequency. Figure 7 presents fluorescence intensity versus frequency with a constant peak applied voltage as a parameter.

From Fig. 7, we can see that as frequency increases, so does fluorescent intensity and thus hydroxyl-radical concentration. The increase in hydroxyl-radical generation/concentration due to the increase in frequency occurs because over a fixed amount of time, there is a higher number of voltage oscillations and, thus, a higher number of breakdowns. To demonstrate, we present four representative samples of applied voltage and currents at the needle electrode in Figs. 8 and 9. The first shows the difference between frequencies of 2 and 6 kHz. The second shows the difference between the frequencies of 10 and 14 kHz.

In Figs. 8 and 9, each peak in the current at the needle electrode represents a plasma discharge. Counting these discharges

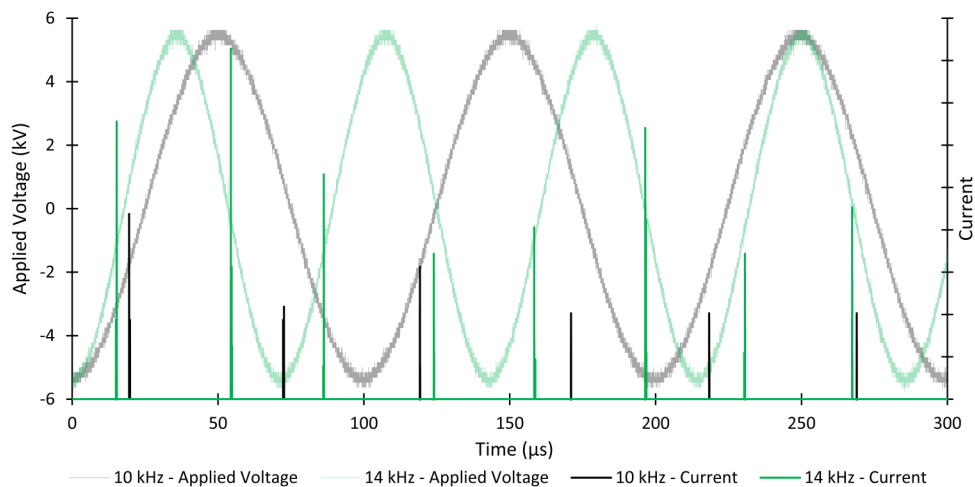


FIG. 9. Current and applied voltage, with respect to ground, at the needle electrode during plasma discharge at 10 and 14 kHz frequencies with constant ± 5 kV peak voltage.

yields approximately 10 700 discharges per second at 2 kHz, 21 600 discharges per second at 6 kHz, 32 000 discharges per second at 10 kHz, and 46 700 per second at 14 kHz. It then follows that if more discharges are being generated in a fixed amount of time the total number of hydroxyl radicals generated should also increase. This will result in an increase in the fluorescence of the plasma-exposed coumarin solution as seen in Fig. 7.

V. SUMMARY AND CONCLUSIONS

In this work, we have shown that coumarin solution, as the liquid in an atmospheric-pressure DBD system, is a useful indicator of hydroxyl-radical concentration if the exposure time is restricted to the monotonic increase region of fluorescence response. Furthermore, it has been shown that hydroxyl-radical generation is dependent on both the frequency and the applied voltage used to generate a DBD plasma. In the case of increasing frequency, this occurs because there are more peak-to-peak voltage oscillations over a set amount of time. Alternatively, when peak applied voltage is increased, it is possible to generate more plasma breakdowns per voltage oscillation. This is due to the potential across the air gap exceeding the dielectric strength of the gas medium multiple times in a single polarity swing. These findings will result in enhanced hydroxyl-radical generation for DBD systems and techniques that employ a liquid electrode. It will also expand their workable ranges by reducing plasma exposure time

and enabling systems that require greater and/or reduced hydroxyl generation.

ACKNOWLEDGMENTS

The authors gratefully acknowledge funding from the following sources: to M.R.S. from DOE (Office of Basic Energy Sciences, Division of Chemical Sciences, Geosciences, and Biosciences, Grant No. DEFG02-88ER13938) and National Science Foundation (NSF) (Molecular and Cellular Biosciences, Grant No. 0929395), and to J.L.S. and M.R.S. jointly from the Wisconsin Alumni Research Foundation (Accelerator Program).

REFERENCES

- ¹Z. Machala and D. B. Graves, *Trends Biotechnol.* **36**, 579 (2018).
- ²B. B. Minkoff, J. M. Blatz, F. A. Choudhury, D. Benjamin, J. L. Shohet, and M. R. Sussman, *Sci. Rep.* **7**, 12946 (2017).
- ³U. Kogelschatz, B. Eliasson, and W. Egli, *J. de Physique IV Colloque* **7**, C4-47 (1997).
- ⁴S. D. Maleknia, M. Brenowitz, and M. R. Chance, *Anal. Chem.* **71**, 3965 (1999).
- ⁵G. Louit, S. Foley, J. Cabillic, H. Coffigny, F. R. Taran, A. Valleix, J. Philippe Renault, and S. Pin, *Radiat. Phys. Chem.* **72**, 119 (2005).
- ⁶P. Attri, Y. H. Kim, D. H. Park, J. H. Park, Y. J. Hong, H. S. Uhm, K.-N. Kim, A. Fridman, and E. H. Choi, *Sci. Rep.* **5**, 9332 (2015).
- ⁷M. J. Pavlovich, T. Ono, C. Galleher, B. Curtis, D. S. Clark, Z. Machala, and D. B. Graves, *J. Phys. D Appl. Phys.* **47**, 505202 (2014).
- ⁸D. W. Fink and W. R. Koehler, *Anal. Chem.* **42**, 990 (1970).